Original Article

Isolating Epidermal Growth Factor Receptor Overexpressing Carcinoma Cells from Human Whole Blood by Bio-Ferrography

Ofer Levi,[1] Assaf Shapira,[2] Baruch Tal,[1] Itai Benhar,[2] and Noam Eliaz[1]*

[1]Biomaterials and Corrosion Lab, Department of Materials Science and Engineering, Tel-Aviv University, Ramat Aviv, Tel Aviv 6997801, Israel

[2]Department of Molecular Microbiology and Biotechnology, Tel-Aviv University, Ramat Aviv, Tel Aviv 6997801, Israel

Background: The epidermal growth factor receptor (EGFR) is overexpressed in carcinoma. In some cases, including in colorectal cancer, it is used as a therapeutic target. Bio-Ferrography is a nondestructive method for isolating magnetized cells and tissues from a fluid onto a glass slide based on their interaction with an external, strong, and focused magnetic field.

Methods: Here, we implement Bio-Ferrography to separate EGFR-positive cancer cells from EGFR-negative noncancer cells, mixed at a ratio of 1 to 1 $\times$ 10^6, from either phosphate-buffered saline or human whole blood. Incubation of the cells with an anti-EGFR antibody and magnetic microbeads coupled to a secondary antibody was used to magnetize the target cells prior to the ferrographic analysis.

Results: A procedure was developed for "a proof of concept" isolation. Recovery values as high as 78% for 1 mL phosphate-buffered saline, and 53% for 1 mL human whole blood, with a limit-of-detection of 30 and 100 target cells, respectively, were achieved.

Conclusions: These capture efficiency values are considered significant and, therefore, warrant further study on isolation of real circulating tumor cells from blood samples of patients, aiming at early diagnosis of EGFR-overexpressing tumor types. © 2014 International Clinical Cytometry Society

Key terms: A431 cells; Bio-Ferrography; EGFR; human whole blood; monoclonal antibody; immunomagnetic separation

How to cite this article: Levi O, Shapira A, Tal B, Benhar I, and Eliaz N. Isolating Epidermal Growth Factor Receptor Overexpressing Carcinoma Cells from Human Whole Blood by Bio-Ferrography. Cytometry Part B 2015; 88B: 136–144.

Colorectal cancer (CRC) is the third most commonly diagnosed cancer (1) and the third leading cause of cancer death. It has also been defined as a high priority for research because of its high occurrence and lack of diagnostic techniques that are both effective and noninvasive.

The disease begins as a benign adenomatous polyp, which develops into an advanced adenoma with high-grade dysplasia, and then progresses to an invasive cancer. Invasive cancers that are confined within the wall of the colon (tumor–node–metastasis Stages I and II) are curable, but if untreated, they spread to regional lymph nodes (Stage III) and then metastasize to distant sites (Stage IV) (2). Advanced CRC is usually treated with combination of chemotherapy (FOLFOX or FOLFIRI) and targeted therapeutics such as anti-epidermal growth factor receptor (EGFR) and anti-vascular endothelial growth factor antibodies or tyrosine kinase inhibitors (3–5). Epithelial cells are the origin of carcinoma cancer types, including CRC. The EGFR is overexpressed in epithelial carcinoma cells. EGFR has been recognized as an important player in CRC initiation and progression, and is even used as a therapeutic target (3–7). Tests routinely used

Additional Supporting Information may be found in the online version of this article.

Correspondence to: N. Eliaz, Biomaterials and Corrosion Lab, Department of Materials Science and Engineering, Tel-Aviv University, Ramat Aviv, Tel Aviv 6997801, Israel. E-mail: neliaz@eng.tau.ac.il

Received 22 July 2014; Revised 15 November 2014; Accepted 24 November 2014

Published online 24 November 2014 in Wiley Online Library (wileyonlinelibrary.com).

DOI: 10.1002/cyto.b.21212

for early CRC detection, such as colonoscopy, flexible sigmoidoscopy, double-contrast barium enema, computed tomography colonography, fecal occult blood test, and stool DNA test, currently suffer from some significant drawbacks (8). For example, the fecal occult blood test and the stool DNA test might overlook some types of CRC. In addition, the former might indicate an exaggerated rate of false positives, whereas the latter is expensive. Once abnormalities are detected by either test, a complementary *in vivo* test (colonoscopy) is required. Given the aforementioned limitations, there is still a need for development of new tests for diagnosis of CRC (8).

Current CRC screening modalities are inadequate for global application because of high costs and a low participation rate. The alternative is to develop a blood-based screening test based on biomarkers that can replace colonoscopy as a first-line screening tool. The blood-based test should identify the high-risk population, which will then be followed by colonoscopy as a secondary test (9). The detection of circulating tumor cells (CTCs) in peripheral blood of patients with resectable colorectal liver metastases or widespread metastatic CRC is associated with disease progression and poor survival (10,11).

Various technologies exist for isolating CTCs from patients' blood samples. Some of them are based on physical characteristics such as size, deformability, density or electric charge, whereas others are based on biological characteristics such as surface protein expression (12). Immunomagnetic isolation (IMI) is based on the expression of proteins on the cell surface. Several IMI-based technologies such as IsoFlux^{TM} (13), OncoCEE^{TM} (12), AdnaTest BreastCancer^{TM} (14), and Precelleon (15) report high recovery values. Yet, the only FDA-approved IMI technology is the CellSearch^{TM} system (16). However, as there is currently no such system in Israel, here we focus on EasySep^{TM} and MACS^{TM} as common IMI technologies with which the results of Bio-Ferrography (BF) are compared.

Analytical ferrography is a nondestructive method of particle separation from a suspension onto a glass slide based upon the interaction between an external magnetic field and the magnetic moments of the particles (17–19). By quantifying the number, shape, size, texture, and composition of particles on the ferrogram (i.e., a microscope slide onto which the captured particles are deposited), the origin, mechanism, and level of wear can be determined.

Several feasibility studies used analytical ferrography in the fields of life sciences and medicine already in the 1980s. These included erythrocyte and white blood cell separation (20–23), bacterial tracking (22–24), and monitoring the wear of either natural diarthrodial joints (25–34) or artificial joints (25,26,29,35). In those studies, Er^{3+} was the magnetizing agent.

BF is the latest modification of the traditional analytical ferrography. BF was specifically developed to allow magnetic isolation of target cells and tissues (19,36,37). Since the introduction of BF in the late 1990s, it has been used in several feasibility studies, which were aimed at tracking *Escherichia coli* bacteria in natural watersheds (38–45), isolation and characterization of low concentrations of *Vibrio cholerae* bacteria from a ships' ballast water (46), capture of magnetic minerals embedded in the comb cells of *Vespinae* (47), isolation of bone and cartilage particles from synovial fluids for early diagnosis of osteoarthritis (48,49), and isolation of both polymeric and metallic wear particles from synovial fluids for either design or failure analysis of artificial hip joints (19,50–52). Some of these studies used antibodies coupled to magnetic microbeads for magnetic labeling of the biological samples (19). The strengths of BF, as demonstrated in these studies, include efficient recovery, high sensitivity, and reasonable analytical errors. Additionally, the ability to characterize microscopically, chemically, and biologically the individual species captured on the ferrogram while preserving the original shape of the species was demonstrated (19). Based on these studies, the necessity to develop a procedure for each application, in particular to optimize the ratios among target cells, bacteria, antibodies, and magnetic microbeads, is evident.

To date, BF has been evaluated only twice in cancer research. Fang et al. (53) used BF to isolate rare MCF-7 breast carcinoma cells from human peripheral leukocytes. The presence of malignant breast cancer cells in bone marrow or peripheral blood was referred to as a prognostic factor. The cell mixture was labeled with an anti-epithelial membrane antigen antibody and a magnetic colloid. The mixtures were prepared in three different ratios between the target and peripheral cells (10^{-4}, 10^{-5}, and 10^{-6}), keeping the number of target cells constant at 30. The recovery value of the MCF-7 cells from the original mixture was about 30%. In the second study (54), BF was applied on samples of $CD4^{+}$ cells in leukocytes and murine lymphoma cells in human peripheral blood. It should be noted that in both cases whole blood was not tested. Furthermore, it was concluded that although BF has good specificity with respect to cell capture, it might not be applicable to rare-event selection because of the inability to capture all available target cells.

In this study, we used an EGFR-based IMI model (55). EGFR is a membrane-bound receptor tyrosine kinase overexpressed and aberrantly activated in a number of epithelial malignancies. It has, therefore, become a key target of therapeutic strategies designed to treat metastatic CRC, for example, with monoclonal antibodies (mAbs) against the extracellular domain of the receptor. Erbitux (Cetuximab) was the first EGFR-specific mAb approved for treatment of CRC. EGFR is expressed not only on epithelial carcinoma cells but also on normal epithelial cells, albeit at much lower levels. In any case, the appearance of epithelial cells in the blood circulation itself is abnormal. The number of EGFR molecules on the surface of tumor cells is on the order of 10^{6} sites per cell (56), which should be sufficiently high to allow their isolation by IMI.

Current clinical early detection tests for carcinoma cancer types, CRC in particular, suffer from some major drawbacks. Moreover, none of the aforementioned IMI

technologies have the capability to concentrate and deposit live CTCs on a glass slide for further theranostic and research applications. Therefore, a BF isolation of immunomagnetic-labeled target cells based on EGFR is suggested in this study. Here, we implemented BF for the first time, as a "proof of concept," for isolating EGFR-overexpressing target cells from human whole blood (HWB).

MATERIALS AND METHODS

A431 and NIH 3T3 Cell Lines

In this study, cells of the A431 epidemoid carcinoma cell line were used as EGFR-overexpressing target cells. They simulate EGFR-overexpressing epithelial CTCs. A431 cells express about 10^6 sites/cell (56). Nontarget cells were modeled by NIH 3T3 mouse embryo fibroblast cells. Bio-ferrographic separation was carried out on either target cells mixed with nontarget cells in phosphate-buffered saline (PBS) or target cells spiked into HWB. Both A431 and 3T3 cell lines were maintained in Dulbecco's Modified Eagle Medium supplemented with 10% fetal calf serum, 2 mM L-glutamine, 100 U/mL penicillin, 100 μg/mL streptomycin, and 12.5 U/mL nystatin (Biological Industries, Israel) in a humidified 5% CO_2 incubator at 37°C. A431 and 3T3 cells were transfected to stably express a red (mCherry) or a green (enhanced green fluorescent protein) fluorescent protein, respectively. The A431 target cells were used in two configurations: either fixed with 4% formaldehyde ("fixed mode") or with no fixation ("unfixed mode").

Human Whole Blood Samples

HWB samples were drawn from blood samples of healthy donors that were tested and supplied by MDA Israel blood services. The use of human blood for this study was approved by the Tel-Aviv University Ethics Committee. To simulate the blood that contains CTCs, the HWB samples were spiked with either 200 or 100 A431 target cells.

Antibodies and Magnetic Microbeads

The IM labeling models in this study are based on high expression of EGFR on the surface of CTCs (and on the model A431 cells) (55,56), the ability of EGFR to be bound by the EGFR-specific antibodies, and the ability of anti-IgG microbeads to bind to the capture antibodies.

Two different IM labeling models were applied in this study. The chimeric anti-EGFR mAb Erbitux was used for the limit-of-detection (LOD) and recovery evaluation experiments (referred hereafter as "human-based Ab model"), whereas a mouse mAb was used for the HWB isolation experiments (referred hereafter as "mouse-based Ab model"). For the first model, Erbitux (Merck KGaA, Darmstadt, Germany; 5 mg/mL solution) was used as the capture antibody to mediate the binding of the target cells (A431) to the magnetic microbeads. Microbeads conjugated to mouse monoclonal anti-human IgG antibodies (Miltenyi Biotec, Auburn, CA) were used for cell isolation. For the second model, EGFR (R-1) mouse anti-human EGFR antibody (Santa Cruz Biotechnology, Santa Cruz, CA, 0.2 mg/mL) was used as the capture antibody. Microbeads conjugated to monoclonal rat-anti-mouse IgG antibodies (Miltenyi Biotec) were used for cell separation.

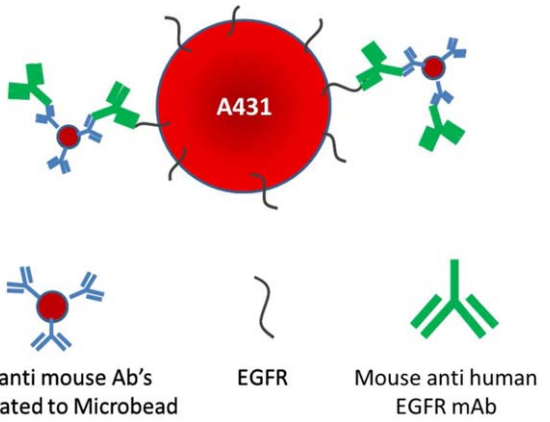

FIG. 1. IM labeling model for human blood samples (mouse-based Ab model). [Color figure can be viewed in the online issue, which is available at wileyonlinelibrary.com.]

IM Labeling Model for LOD and Recovery Evaluation (Human-Based Antibody Model)

A431 target cells were suspended in PBS in varying numbers ranging from 1×10^5 down to 30. The samples were incubated with Erbitux (in excess relatively to the binding capacity of the cells) at a final concentration of 900 nM, shaken for 1–2 h at room temperature (RT), followed by two washing steps in order to remove the excess amount of unbound antibodies. The washing steps included two steps of sample centrifugation at 300*g*, at 4°C for 10 min, careful removal of the cell-free supernatant, and adding PBS to bring the sample back to its original volume. Next, the samples were incubated with 20 μL microbeads for at least 15 min at 7°C while shaking frequently. Two additional washing steps were then carried out before BF separation.

IM Labeling Model for Human Blood Samples (Mouse-Based Ab Model)

Samples of 1 mL HWB were spiked with varying numbers of fixed or unfixed A431 target cells. The samples were centrifuged twice and washed. Subsequently, 0.3 mL of a "cocktail suspension" comprising 333 nM capture mAb (EGFR(R-1)) preincubated with 20 μL microbeads for at least 15 min at 7°C were added to the samples. The HWB samples were incubated with the cocktail suspension for 1–2 h using an orbital shaker at 50 rpm at RT. The samples were washed twice with PBS before BF separation. This model is illustrated in Figure 1.

Isolating Target Cells on the Bio-Ferrograph

In this study, Bio-Ferrograph 2100 (Guilfoyle, Belmont, MA) (19,36) was used. This is a bench-top cytometry-

based instrument (Supporting Information Fig. S1). It utilizes a magnetic field that has maximal field strength across an interpolar gap, where the collection of magnetically susceptible particles takes place (Fig. S1). Because the gradient of that field is maximal at the edges of the gap, two parallel deposition strips (primary and secondary) are formed, and a rectangular deposition band can be observed on the ferrogram even by naked eye. A very high magnetic flux is established at the interpolar gap. The vertical flow separates the vertical gravitational force from the nearly horizontal magnetic force so that only the latter acts to retain magnetic particles moving downward through a flow chamber of 16 mm $\times$ 6 mm $\times$ 0.5 mm.

For BF, the samples were labeled with capture antibodies and magnetic microbeads and washed twice, as described earlier. The sample tubes were filled to a constant volume of 0.5 mL with PBS. The BF isolation process was initiated by filling the capture cell and the reservoir with 0.5 mL PBS at a flow rate of 0.1 mL/min. The samples with the labeled target cells were inserted into the reservoir. They were then flowed over the capture band at a rate of 0.05 mL/min, followed by washing with PBS at the same flow rate. The slide with the captured cells was separated from the BF cassette and examined under an inverted microscope (Olympus model IX71, Tokyo, Japan) using the fluorescence and bright-field modes for identifying and counting the captured cells.

Experiments with the Human Model

To validate the expression of EGFR on the A431 target cells, they were incubated in 10% bovine serum for 1 h to block nonspecific binding sites. Cells were subsequently incubated with 180 nM Erbitux for 1 h, or without Erbitux (negative control samples). All samples were washed twice, and fluorescein isothiocyanate-labeled goat-anti-human antibody (Jackson Immuno Research Laboratories, West Grove, PA; 1.5 mg/mL) was added as a secondary Ab at a final concentration of 200 nM. Following 1 h incubation, two washing steps were applied. The cells were spotted on microscope slides and examined under an inverted microscope (Olympus IX71) using the fluorescence and bright field modes.

To evaluate the feasibility of capturing target cells by BF, a mixture of 3×10^6 3T3 background cells expressing enhanced green fluorescent protein and 3×10^5 A431 target cells expressing mCherry were suspended in 240 μL of PBS (Solution A). A volume of 70 μL of microbeads suspension was mixed with 340 nM Erbitux solution (thus forming Solution B). The amount of Erbitux was defined; so, the mixture of Solutions A and B would contain at least 1×10^9 antibody molecules per target cell. This amount of antibody molecules was three orders of magnitude higher than the amount of EGFR binding sites that appear on each cell (57). Each solution was incubated for 1 h at RT. Solution A was then divided into three 80 μL aliquots; to each one, 20 μL of Solution B was added. The samples were then run on the Bio-Ferrograph.

Evaluation of Bio-Ferrography LOD and Recovery Values

To establish a robust working protocol, BF LOD and recovery values were specified. The LOD was set as 30 target cells, and the recovery values were determined for samples with 30 target cells in the absence of background cells or in the presence of 30×10^6 background cells. Several parameters were adjusted, and the following labeling and isolating conditions were applied: Erbitux final concentration of 900 nM, 20 μL of microbeads, and sample volume of 300 μL. The tubes were left at 7°C for 1 h with occasional mixing (every 15 min). The samples were spun at 300*g* for 10 min at 4°C, followed by two washes. The flow capture rate on the BF was set at 0.05 mL/min.

The LOD values were set per 1 mL of either PBS or HWB, and the recovery values were calculated according to Eq. (1):

$$\text{Recovery}\,[\%] = \frac{\text{The number of captured cells}}{\text{The number of spiked cells}} \times 100 \quad (1)$$

The inlet numbers of target cells were evaluated as an average value of counted target cells that were sedimented in two drops from the cell suspension on a cover slip. Florescent microscopy was used for cell counting.

For morphologic observation, slides were stained by the Diff-Quik method. The slides were fixed for 2 sec with methanol, followed by washing with distilled water. Afterward, the slides were dipped for 2 sec in eosin, followed by washing with distilled water. Finally, the slides were dipped in hematoxilyn for 1 min, followed by additional washing with distilled water.

Comparison with Other IMI Technologies

The results obtained by BF were compared, side by side, by analyzing the same samples using two common IMI technologies: MACS (Miltenyi Biotec, Bergisch-Gladbach, Germany) and EasySep (Stemcell Technologies, Vancouver, BC, Canada). Both technologies are used for "negative" and "positive" cell separation. However, the former applies a magnetic field on a flowing sample in a porous medium, whereas the latter is done on an immobile sample.

In addition to the tested IMI technologies, we considered the CellSearch system (Janssen Diagnostics BVBA, Beerse, Belgium). This is the only FDA-approved IM method for detecting CTCs. Unfortunately, such system is currently not available in Israel. Therefore, its evaluation will be made based on published data in the Discussion section.

Samples containing 1×10^5 target cells were IM labeled (human-based Ab model). In EasySep, each sample was exposed to the magnetic field according to the EasySep Human Cell Isolation Protocol and was subsequently transferred into the kit's swap tube. The captured cells were washed from the tube wall, and a volume of 10 μL was subsequently analyzed by light microscopy at ×100 magnification. For MACS tests, the mini size configuration of column tubes and magnet

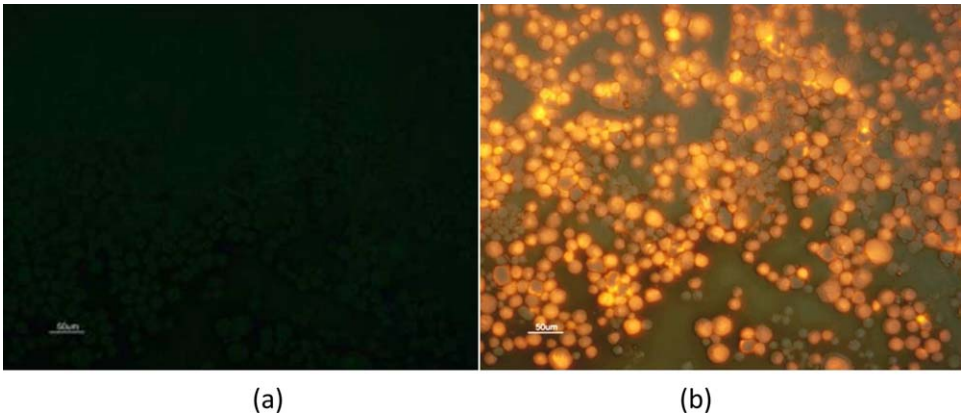

FIG. 2. Fluorescence microscopy images demonstrating no background cells (**a**) and numerous captured target cells (**b**) on the ferrogram in Experiment #1. Bar = 50 μm. [Color figure can be viewed in the online issue, which is available at wileyonlinelibrary.com.]

(MiniMACS^{TM} Separator and MiniMACS Starting Kit (MS)) was used according to Miltenyi Biotec protocol for human-anti-IgG microbeads. The MACS column tube was washed with buffer. The suspension that passed through the column tube was collected in the kit's "−neg. tube," whereas the cells that were captured in the column were collected in a "+pos. tube."

Experiments with the Mouse-Based Ab Model: Recovery of Target Cells from Human Whole Blood

In this model, a mouse-anti-human EGFR antibody and rat-anti-mouse immunomagnetic microbeads were used. Two comparative experiments were carried out to examine the differences between the captured sample components while converting the human-based Ab IM labeling model to the mouse-based Ab IM labeling model.

Six samples of 1 mL HWB each were spiked with 200 fixed or 100 unfixed target cells. The samples were washed and were IM labeled (three samples were labeled with a mouse-based Ab cocktail suspension, whereas the other three samples with a human-based Ab cocktail suspension), followed by the isolation procedure on the BF as described above.

RESULTS

Target Cells Express EGFR

In preliminary experiments (data not included herein), we found that in order to efficiently capture up to 10^4 target cells with minimal or no capture of nontarget cells, Erbitux (the capture antibody) should be used at a final concentration of 180 nM. To verify that the target cells express EGFR, two samples containing 1×10^4 target cells—one incubated with 180 nM Erbitux and the other without—were compared under a fluorescence microscope after incubation with a fluorescein isothiocyanate-labeled secondary antibody. As shown in Supporting Information Figure S2, the cells were brightly stained.

Target Cells Can Be Captured by BF

For feasibility tests, mixtures of 3×10^5 fixed target cells and 3×10^6 fixed background cells were IM labeled and isolated by the BF. A brown sediment (of microbeads) within the rectangular deposition band of the BF slide (the ferrogram) could be observed by naked eye (not shown). As shown in Figure 2a, no background

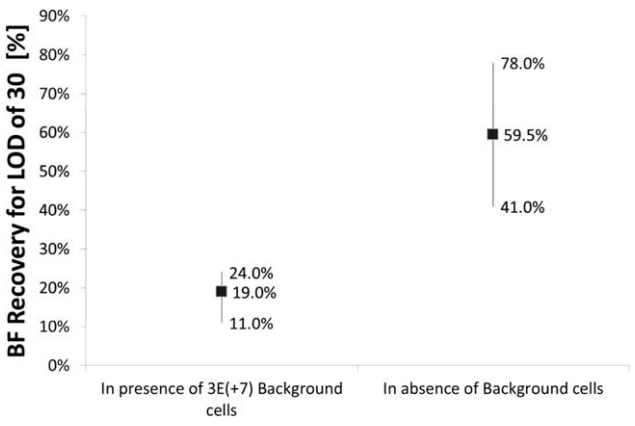

FIG. 3. The BF recovery values for LOD = 30 target cells.

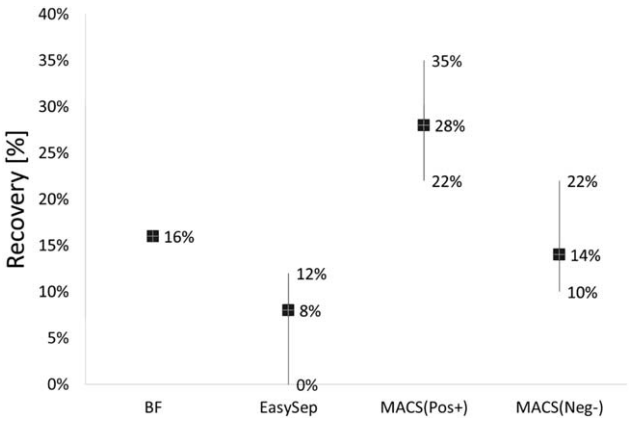

FIG. 4. The recovery values of MACS^{TM} (Pos $n = 4$; Neg $n = 4$), BF ($n = 2$), and EasySep^{TM} ($n = 3$).

cells were observed under the fluorescence microscope. In contrast, as shown in Figure 2b, numerous target cells could be observed. Images representative of the three deposition channels on the ferrogram demonstrated repeatability. Thus, it was concluded that the target cells can be successfully separated from the background cells under these conditions.

The BF LOD and Recovery Values

The LOD was set as 30 A431 target cells either in the absence or in the presence of 30×10^6 3T3 background cells. Figure 3 presents the recovery values for LOD of 30 target cells. It is evident that the presence of background cells in the sample undergoing IMI caused a significant reduction in the recovery values (from 41%–78% to 11%–24%).

Comparison with Other IMI Techniques

The results obtained by BF were compared with those obtained in this study by two common IMI technologies: MACS and EasySep. MACS and EasySep isolations were carried out using 10^5 target cells as input, with no background cells. EasySep revealed 3, 0, and 3 cells by hemocytometry in three different samples, respectively. These values correspond to cell numbers of 12,000, 0, and 12,000 in the entire sample (from an input of 1×10^5 cells), respectively, representing recovery values of 0%–12% (Fig. 4). MACS revealed recovery values of 25%–35% in two samples (Fig. 4). Two BF experiments that were carried out in parallel, using an identical target cell input, resulted in a very high (uncountable) number of captured cells in most of the channels. The captured cells formed a fairly uniform deposition band in each channel. Based on comparison with other ferrograms, the number of captured cells was roughly estimated at the thousands scale.

For a quantitative comparison, we carried out the BF analysis using a lower number of target cells (10^4), which allows the calculation of recovery values. The BF experiments still yielded an uncountable number of captured target cells in those channels. However, a rough estimation of more than 2,000 cells (corresponding to a recovery value of at least 16%) was made in the two different BF runs. The results obtained from the three techniques are compared in Figure 4.

BF Can Be Used to Recover Target Cells from HWB

The mouse-based Ab model revealed significantly higher recovery values than the human-based Ab model. With this model, when about 230 fixed target cells were used as input, the recovery value was 49% ± 4.9%. When about 100 unfixed target cells were used as input, the recovery value was 42.0% ± 11.5%. Figure 5 presents the capture cell downstream and the target cells isolated from HWB in the capture band.

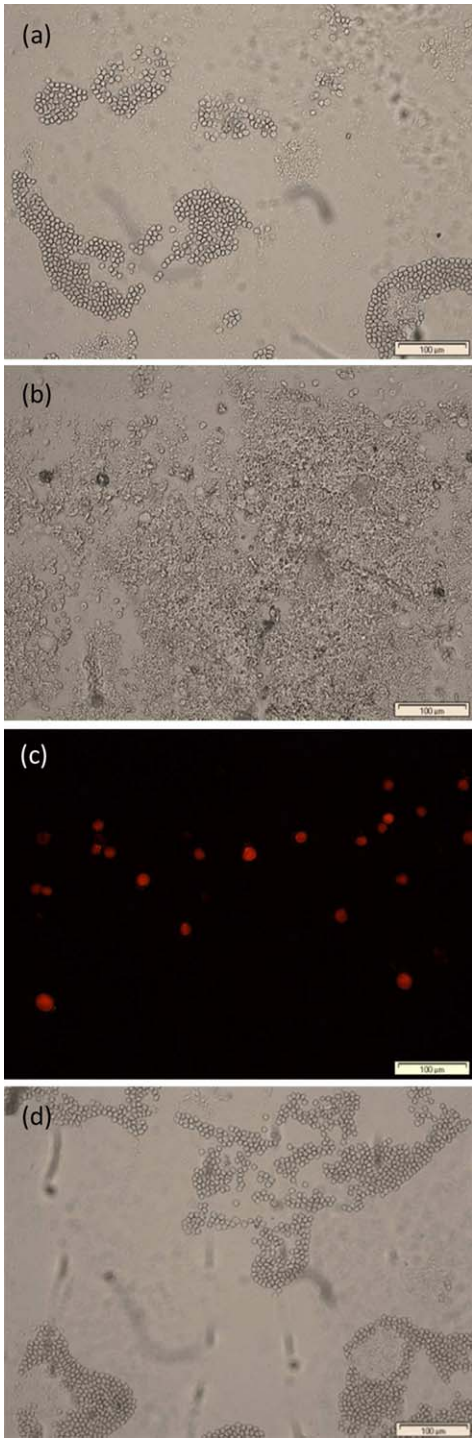

FIG. 5. Light microscopy images of captured cells in a mouse-based Ab model, fixed-cell experiment. (**a**) Bright-field image from above the capture band (upstream). (**b**) Bright-field image from within the capture band. (**c**) Red fluorescence image of the captured cells within the capture band. (**d**) Bright-field image from below the capture band (downstream). [Color figure can be viewed in the online issue, which is available at wileyonlinelibrary.com.]

DISCUSSION

Specific and sensitive detection of CTCs is highly desirable in the field of cancer diagnostics. An ideal technology should be able to detect a small number of antigen-positive cells on the background of whole blood in a small volume representing a blood sample obtained in the clinic. This

Table 1
Comparison Between the Characteristics of the Three IMI Technologies

Feature	EasySep™	MACS™	CellSearch™	BF
LOD per 1 mL sample volume	1×10^5	1×10^5	Few	30
Process multiple samples simultaneously				√
Analyzing a large number of cells	√	√	√	
Analyzing various captured cells simultaneously				√
Capture cells in a defined array			√	√
Preserve cell morphology	√	√	√	√
Typical sample size	1 mL	1 mL	7.5 mL	1 mL
IM models adjustable		√		√
Complementary morphological analysis				√
Cost per sample (US$)	Cheapest	Cheaper	800	150
Potential cell loss due to sample transfer	++	+++	++	+
Automated process	No	No	Semiautomated	No

study was carried out to evaluate the feasibility of BF to serve as a tool for EGFR-overexpressing CTCs detection and to provide a comparison with other more commonly used magnetic cell isolation technologies.

Although the experiments presented here are for isolating target cells by BF as a "proof of concept" only, significant recovery values for a very low LOD were achieved. The BF recovery values obtained in this study were 41%–78% from 1 mL of PBS for an LOD of 30 fixed cells, and 31%–53% from 1 mL HWB for an LOD of 100 unfixed cells.

This achievement became possible following an identification of the process parameters that affect the recovery values, for example, incubation volume, incubation time, flow rate, number of washes, etc. (data not shown). Initially, we validated that the A431 cells we used indeed express EGFR on their surface at a level that allows their efficient capture. Next, using the chimeric anti-EGFR antibody Erbitux and immunomagnetic microbeads coupled to anti-human antibodies, we demonstrated an ability to efficiently capture target cells from buffer at a high efficiency, as high as 78% with an LOD of as few as 30 target cells.

Although we have used BF before for various applications (19,47–49,51,52), these applications did not include capture of (cancer) cells. Thus, it was decided to minimize the risk by using a human model that combines Cetuximab (Erbitux)—an FDA-approved therapeutic antibody, which is a very specific anti-EGFR antibody—and the A431 model cell line, which represents cells with high number (10^6) of EGFR sites per cell.

The transition from a human-based Ab IM labeling model to a mouse-based Ab labeling model led to a significant increase in the recovery value. When a human-based Ab IM labeling model was used to capture target cells spiked into HWB, the recovery values were very low, around 16% (data not shown). Using the mouse-based Ab IM labeling model with an LOD of 200 fixed or 100 unfixed target cells in HWB, the recovery values increased to 49% and 42%, respectively. To the best of our knowledge, this is the first report on the use of BF for capturing cells from whole blood.

A comparison is made in this study between BF, EasySep and, MACS. When using high numbers of target cells (on the order of 10^5), the high recovery of BF resulted in the number of captured cells being too high to be counted. Yet, this input number of target cells was too low for obtaining reproducible, statistically significant results by EasySep. MACS was found applicable and, in some cases, yielded higher recovery values than BF. However, when dealing with low numbers of target cells (i.e., as low as 30), the strength of BF compared with EasySep and MACS became significant. Table 1 summarizes the capabilities of all three technologies. BF was found preferable than EasySep and MACS, especially in isolating a small number of target cells.

Other IMI-based technologies not tested here include IsoFlux, OncoCEE, AdnaTest BreastCancer, and CellSearch. The latter is the only FDA-approved technique to-date. Unfortunately, its availability outside the continental USA is low. The absence of such system in Israel prevented us from carrying out comparative tests by BF and CellSearch. The strengths of the latter include high sensitivity, specificity, and reproducibility. Being commercially available and approved by the FDA, it is currently used in many clinical studies that involve a large number of patients. Nevertheless, literature survey and private communications revealed two major disadvantages of CellSearch compared with BF: (1) it is expensive for widespread application, and (2) subsequent morphological and molecular analyses are impossible; thus, the doctors in the clinics often find it difficult to translate its output to practical decisions.

The estimated cost of a single sample by BF is $150. In contrast, the analysis of a single sample by CellSearch costs approximately 80,000 yen ($800). Moreover, because the anticancer and molecular targeting drugs currently given to patients with metastatic CRC as the standard therapy are expensive, repeated use of the CellSearch system will increase the patients' economic burden (58).

Researchers have reached an important consensus that cytopathologic examination of CTCs after immunomagnetic enrichment, with further characterization of their malignant potential, represents a promising approach (59–62). For example, the validation of isolated cells such as CTCs can be corroborated by identifying certain morphological characteristics of the cell. From this point of view, several criteria for CTC

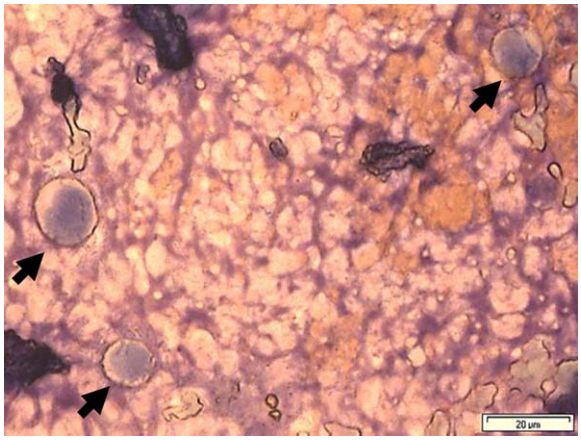

FIG. 6. Three captured cells (arrows) within the capture band on a ferrogram stained by Diff-Quik. The cytoplasm and nucleus condition can be clearly noticed, the cell and nucleus size can be measured, and the cytoplasm-to-nucleus size ratio can be calculated. [Color figure can be viewed in the online issue, which is available at wileyonlinelibrary.com.]

identification were agreed upon: the cytoplasm condition, irregular nuclear membrane, large size of nucleus (larger than 24 μm), anisonucleosis (ratio > 0.5), an increased nucleo-cytoplasmic ratio, and the presence of grouped cells (63). Morphological analysis may also provide specific information on the primary tumor type.

CellSearch positive detection is based on the appearance of cytokeratins 8, 18, or 19. Several studies have shown cytokeratins to be expressed in samples from both healthy volunteers and patients with hematologic malignancies, yielding false-positives (63). A complimentary morphological analysis capability, such as the one that BF offers, can overcome this detection limitation. Figure 6 presents morphological information that can be derived from captured A431 cells on a BF slide stained by Diff-Quik. The feasibility of imaging rare circulating endothelial cells by imaging flow cytometry without the need for any pre-enrichment processes has only recently been demonstrated and published in this *journal* (64).

This work was aimed to demonstrate the isolation of specific models by BF as a "proof of concept." The important advantage of the BF technique is that it concentrates the target cells on a slide, thus making downstream processing of the captured cells at the single-cell level straightforward. The experiments presented here were carried out as a "proof of concept" for the ability of BF to capture EGFR-positive target cells in HWB. We believe that the recovery values can be further improved by further optimizing the IM labeling and isolating parameters such as mAb and microbead concentrations and incubation conditions.

The aforementioned values demonstrate that separating EGFR-overexpressing CTCs can be done by BF. Although the recovery values are lower than those reported for CellSearch and IsoFlux, the process presented here is for "proof of concept" only, and may be used as a starting point for comprehensive optimization prior to clinical application.

CONCLUSIONS

This study demonstrates the applicability of BF in the isolation of EGFR-positive tumor cells from HWB, as a "proof of concept." The fact that A431 cells, which express a high level of EFGR, were used as target cells in this study could make this novel technology applicable for other EGFR-overexpressing epithelial CTCs. The recovery values for the lower LOD in HWB may open a path for the use of BF as a monitoring tool, or could even be used for early cancer detection in patients in the future.

ACKNOWLEDGMENTS

The authors thank MADA blood services for their cooperation and support. They thank Prof. Dan Peer and his research group members at the Faculty of Life Sciences, Tel-Aviv University, for their technical support with the EasySep and hemocytometry.

LITERATURE CITED

1. American Cancer Society. Cancer Facts & Figures 2013. Atlanta, GA: American Cancer Society; 2013.
2. Sanford D, Markowitz MD, Monica MB. Molecular origins of cancer: Molecular basis of colorectal cancer. N Engl J Med 2009;361:2449–2460.
3. Ahmed S, Johnson K, Ahmed O, Iqbal N. Advances in the management of colorectal cancer: From biology to treatment. Int J Colorectal Dis 2014;29:1031–1042.
4. Hohla F, Winder T, Greil R, Rick FG, Norman L. Targeted therapy in advanced metastatic colorectal cancer: Current concepts and perspectives. World J Gastroenterol 2014;20:6102–6112.
5. Grávalos C1, Cassinello J, Fernández-Rañada I, Holgado E. Role of tyrosine kinase inhibitors in the treatment of advanced colorectal cancer. Clin Colorectal Cancer 2007;6:691–699.
6. Duffy MJ, Lamerz R, Haglund C, Nicolini A, Kalousova M, Holubec L, Sturgeon C. Tumor markers in colorectal cancer, gastric cancer and gastrointestinal stromal cancers: European group on tumor markers 2014 guidelines update. Int J Cancer 2014;134:2513–2522.
7. Sihver W, Pietzsch J, Krause M, Baumann M, Steinbach J, Pietzsch H-J. Radiolabeled Cetuximab conjugates for EGFR targeted cancer diagnostics and therapy. Pharmaceuticals 2014;7:311–338.
8. American Cancer Society. Colorectal Cancer Facts & Figures 2011–2013. Atlanta, GA: American Cancer Society; 2011.
9. Ganepola AP, Nizin J, Rutledge JR, Chang DH. Use of blood-based biomarkers for early diagnosis and surveillance of colorectal cancer. World J Gastrointest Oncol 2014;6:83–97.
10. Koerkamp BG, Rahbari NN, Büchler MW, Koch M, Weitz J. Circulating tumor cells and prognosis of patients with resectable colorectal liver metastases or widespread metastatic colorectal cancer: A meta-analysis. Ann Surg Oncol 2013;20:2156–2165.
11. Sastre J, Maestro ML, Puente J, Veganzones S, Alfonso R, Rafael S, García-Saenz JA, Vidaurreta M, Martín M, Arroyo M, et al. Circulating tumor cells in colorectal cancer: Correlation with clinical and pathological variables. Ann Oncol 2008;19:935–938.
12. Hong B, Zu Y. Detecting circulating tumor cells: Current challenges and new trends. Theranostics 2013;3:377–394.
13. Harb W, Fan A, Tran T, Danila DC, Keys D, Schwartz M, Ionescu-Zanetti C. Mutational analysis of circulating tumor cells using a novel microfluidic collection device and qPCR assay. Transl Oncol 2013;6:528–538.
14. Van der Auwera I, Peeters D, Benoy IH. Circulating tumor cell detection: A direct comparison between the CellSearch system, the AdnaTest and CK-19/mammaglobin RT–PCR in patients with metastatic breast cancer. Br J Cancer 2010;102:276–284.
15. Wu Y, Deighan CJ, Miller BL, Balasubramanian P, Lustberh MB, Zborowski M, Chalmers JJ. Isolation and analysis of rare cells in the blood of cancer patients using a negative depletion methodology. Methods 2013;64:169–182.
16. Allard WJ, Matera J, Miller MC, Repollet M, Connelly MC, Rao C, Tibbe AGJ, Uhr JW, Terstappen LWMM. Tumor cells circulate in the peripheral blood of all major carcinomas but not in healthy subjects

or patients with nonmalignant diseases. Clin Cancer Res 2004;10: 6897–6904.
17. Seifert WW, Westcott VC. A method for the study of wear particles in lubricating oil. Wear 1972;21:27–42.
18. Levi O, Eliaz N. Failure analysis and condition monitoring of an open-loop oil system using Ferrography. Tribol Lett 2009;36:17–29.
19. Eliaz N, Hakshur K. Fundamentals of tribology and the use of ferrography and bio-ferrography for monitoring the degradation of natural and artificial joints. In: Eliaz N, editor. Degradation of Implant Materials. New York: Springer; 2012. pp 253–302.
20. Hunter JA, Mills GH, Sturrock RD. Ferrography: A new method for isolation of particles from biological fluids. J Clin Pathol 1982;35: 689–690.
21. Graham MD, Selvin PR. Separation of lanthanide binding cells. IEEE Trans Magn 1982;18:1523–1525.
22. Russell AP, Westcott VC, Demaria A, Johns M. The concentration and separation of bacteria and cells by ferrography. Wear 1983;90: 159–165.
23. Jones WR. Wear Particle Analysis Using the Ferrograph. NASA Technical Memorandum 83422. Cleveland, OH: NASA Glenn Research Center; 1983.
24. Zborowski M, Malchesky PS, Savon SR, Green R, Hall GS, Nosé Y. Modification of ferrography method for analysis of lymphocytes and bacteria. Wear 1991;142:135–149.
25. Mears DC, Hanley EN, Rutkowski R, Westcott VC. Ferrography: Its application to the study of human joint wear. Wear 1978;50:115–125.
26. Evans CH, Mears DC. The wear particles of synovial fluid: Their ferrographic analysis and pathophysiological significance. Bull Prosthet Res 1981;Fall:13–26.
27. Evans CH, Mears DC, McKnight JL. A preliminary ferrographic survey of the wear particles in human synovial fluid. Arthritis Rheum 1981;24:912–918.
28. Evans CH, Mears DC, Stanitski CL. Ferrographic analysis of wear in human joints. Evaluation by comparison with arthroscopic examination of symptomatic knees. J Bone Joint Surg Br 1982;64:572–578.
29. Evans CH. Application of ferrography to the study of wear and arthritis in human joints. Wear 1983;90:281–292.
30. Mills GH, Hunter JA. A preliminary use of ferrography in the study of arthritic diseases. Wear 1983;90:107–111.
31. Podsiadlo P, Kuster M, Stachowiak GW. Numerical analysis of wear particles from non-arthritic and osteoarthritic human knee joints. Wear 1997;210:318–325.
32. Stachowiak GW, Podsiadlo P. Analysis of wear particle boundaries found in sheep knee joints during in vitro wear tests without muscle compensation. J Biomech 1997;30:415–419.
33. Kuster MS, Podsiadlo P, Stachowiak GW. Shape of wear particles found in human knee joints and their relationship to osteoarthritis. Br J Rheumatol 1998;37:978–984.
34. Graindorge SL, Stachowiak GW. Changes occurring in the surface morphology of articular cartilage during wear. Wear 2000;241:143–150.
35. Mears DC, Hanley EN, Rutkowski R, Westcott VC. Ferrographic analysis of wear particles in arthroplastic joints. J Biomed Mater Res 1978;12:867–875.
36. Guilfoyle, Inc. New on the market: Bio-Ferrograph 2100. Nature 2000;407:818.
37. Parkansky N, Alterkop B, Boxman RL, Leitus G, Berkh O, Barkay Z, Rosenberg Yu, Eliaz N. Magnetic properties of carbon nano-particles produced by a pulsed arc submerged in ethanol. Carbon 2008;46: 215–219.
38. Zhang P, Johnson WP. Rapid selective ferrographic enumeration of bacteria. J Magn Mater 1999;194:267–274.
39. Zhang P, Johnson WP, Rowland R. Bacterial tracking using ferrographic separation. Environ Sci Technol 1999;33:2456–2460.
40. Johnson WP, Zhang P, Fuller ME, Scheibe TD, Mailloux BJ, Onstott TC, DeFlaun MF, Hubbard SS, Radtke J, Kovacik WP, et al. Ferrographic tracking of bacterial transport in the field at the Narrow Channel Focus Area, Oyster, VA. Environ Sci Technol 2001;35:182–191.
41. Johnson WP, Zhang P, Gardner PM, Fuller ME, DeFlaun MF. Evidence for detachment of indigenous bacteria from aquifer sediment in response to arrival of injected bacteria. Appl Environ Microbiol 2001;67:4908–4913.
42. Fuller M, Mailloux B, Zhang P, Streger SH, Hall JA, Vainberg SN, Beavis AJ, Johnson WP, Onstott TC, DeFlaun MF. Field-scale evaluation of CFDA/SE staining coupled with multiple detection methods for assessing the transport of bacteria in situ. FEMS Microbiol Ecol 2001;37:55–66.
43. DeFlaun MF, Fuller ME, Zhang P, Johnson WP, Mailloux B, Holben WE, Kovacik WP, Balkwill DL, Onstott TC. Comparison of methods for monitoring bacterial transport in the subsurface. J Microbiol Methods 2001;47:219–231.
44. Zhang P, Johnson WP, Scheibe TD, Choi K, Dobbs FC. Extended tailing of bacteria following breakthrough at the Narrow Channel Focus Area, Oyster, Virginia. Water Resource Res 2001;37:2687–2698.
45. Johnson WP, McIntosh OW. Tracking of injected and resident (previously injected) bacterial cells in groundwater using ferrographic capture. Microbiol Methods 2003;54:153–164.
46. Drake LA, Meyer AE, Forsberg RL, Baier RE, Doblin MA, Heinemann S, Johnson WP, Koch M, Rublee PA, Dobbs FC. Potential invasion of microorganisms and pathogens via 'interior hull fouling': Biofilms inside ballast water tanks. Biol Invasions 2005;7:969–982.
47. Ishay JS, Barkay Z, Eliaz N, Plotkin M, Volynchik S, Bergaman DJ. Gravity orientation in social wasp comb cells (Vespinae) and the possible role of embedded minerals. Naturwissenschaften 2008;95: 333–342.
48. Mendel K, Eliaz N, Benhar I, Hendel D, Halperin N. Magnetic isolation of particles suspended in synovial fluid for diagnostics of natural joint chondropathies. Acta Biomater 2010;6:4430–4438.
49. Hakshur K, Benhar I, Bar-Ziv Y, Halperin N, Segal D, Eliaz N. The effect of hyaluronan injections into human knees on the number of bone and cartilage wear particles captured by bio-ferrography. Acta Biomater 2011;7:848–857.
50. Meyer DM, Tillinghast A, Hanumara NC, Franco A. Bio-ferrography to capture and separate polyethylene wear debris from hip simulator fluid and compared with conventional filter method. J Tribol 2006;128:436–441.
51. Elsner JJ, Mezape Y, Hakshur K, Shemesh M, Linder-Ganz E, Shterling A, Eliaz N. Wear rate evaluation of a novel polycarbonate-urethane cushion form bearing for artificial hip joints. Acta Biomater 2010;6:4698–4707.
52. Elsner JJ, Shemesh M, Mezape Y, Levenshtein M, Hakshur K, Shterling A, Linder-Ganz E, Eliaz N. Long-term evaluation of a compliant cushion form acetabular bearing for hip joint replacement: A 20 million cycles wear simulation. J Orthop Res 2011;29:1859–1866.
53. Fang B, Zborowski M, Moore LR. Detection of rare MCF-7 breast carcinoma cells from mixture of human peripheral leukocytes by magnetic deposition analysis. Cytometry 1999;36:294–302.
54. Turpen PB. Isolation of cells using bioferrography. Cytometry 2000; 42:324.
55. Baselga J. The EGFR as a target for anticancer therapy—Focus on Cetuximab. Eur J Cancer 2001;37:S16–S22.
56. Derer S, Bauer P, Lohse S, Scheel AH, Berger S, Kellner C, Peipp M, Valerius T. Impact of epidermal growth factor receptor (EGFR) cell surface expression levels on effector mechanisms of EGFR antibodies. J Immunol 2012;189:5230–5239.
57. Chen YW, Chiang PJ. Automatic cell counting for hemocytometers through image processing. World Acad Sci Eng Technol 2011;58: 719–722.
58. Sato N, Hayashi N, Imamura Y, Tanaka Y, Kinoshita K, Kurashige J, Saito S, Karashima R, Hirashima K, Nagai Y, et al. Usefulness of transcription–reverse transcription concerted reaction method for detecting circulating tumor cells in patients with colorectal cancer. Ann Surg Oncol 2012;19:2060–2065.
59. Cristofanilli M, Budd GT, Ellis MJ, Stopeck A, Matera J, Miller MC, Reuben JM, Doyle GV, Allard WJ, Terstappen LWMM, et al. Circulating tumor cells, disease progression, and survival in metastatic breast cancer. N Engl J Med 2004;351:781–791.
60. Cristofanilli M, Hayes DF, Budd GT, Ellis MJ, Stopeck A, Reuben JM, Doyle GV, Matera J, Allard WJ, Miller MC, et al. Circulating tumor cells: A novel prognostic factor for newly diagnosed metastatic breast cancer. J Clin Oncol 2005;23:1420–1430.
61. Cristofanilli M, Mendelsohn J. Circulating tumor cells in breast cancer: Advanced tools for "tailored" therapy. Proc Natl Acad Sci USA 2006;103:17073–17074.
62. Armakolas A, Panteleakou Z, Nezos A, Tsouma A, Skondra M, Lembessis P, Pissimissis N, Koutsilieris M. Detection of the circulating tumor cells in cancer patients. Future Oncol 2010;6:1849–1856.
63. Miron N, Susman S, Balacescu O, Buiga R, Berindan-Neagoe I, Cristea V, Balacescu L, Manolescu V, Eliade Ciuleanu T. Novel cellular and molecular approaches to stratification and treatment of colorectal cancer. J Gastrointestin Liver Dis 2012;21:413–421.
64. Samsel L, Dagur PK, Raghavachari N, Seamon C, Kato GJ, McCoy JP. Imaging flow cytometry for morphologic and phenotypic characterization of rare circulating endothelial cells. Cytometry Part B 2013; 84B:379–389.

Supplementary information

Supplementary Figures

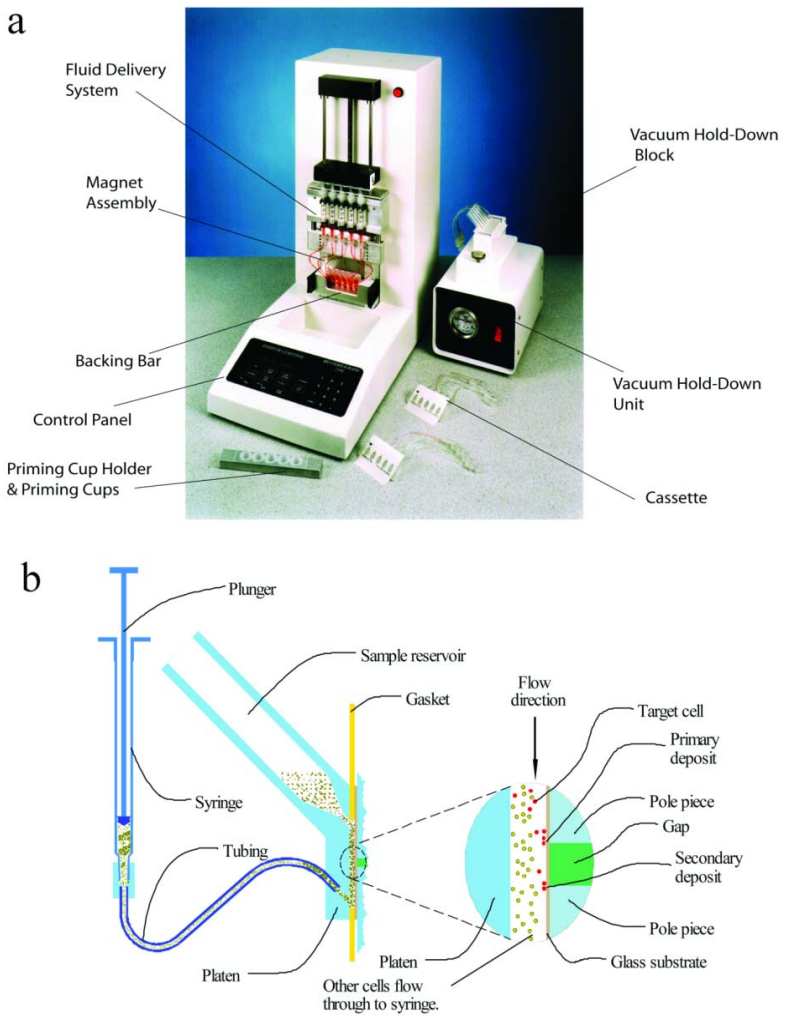

Fig.S1. (a) The components of Bio-Ferrograph 2100 (Guilfoyle, Inc.). (b)The deposition scheme of captured particles on the slide.

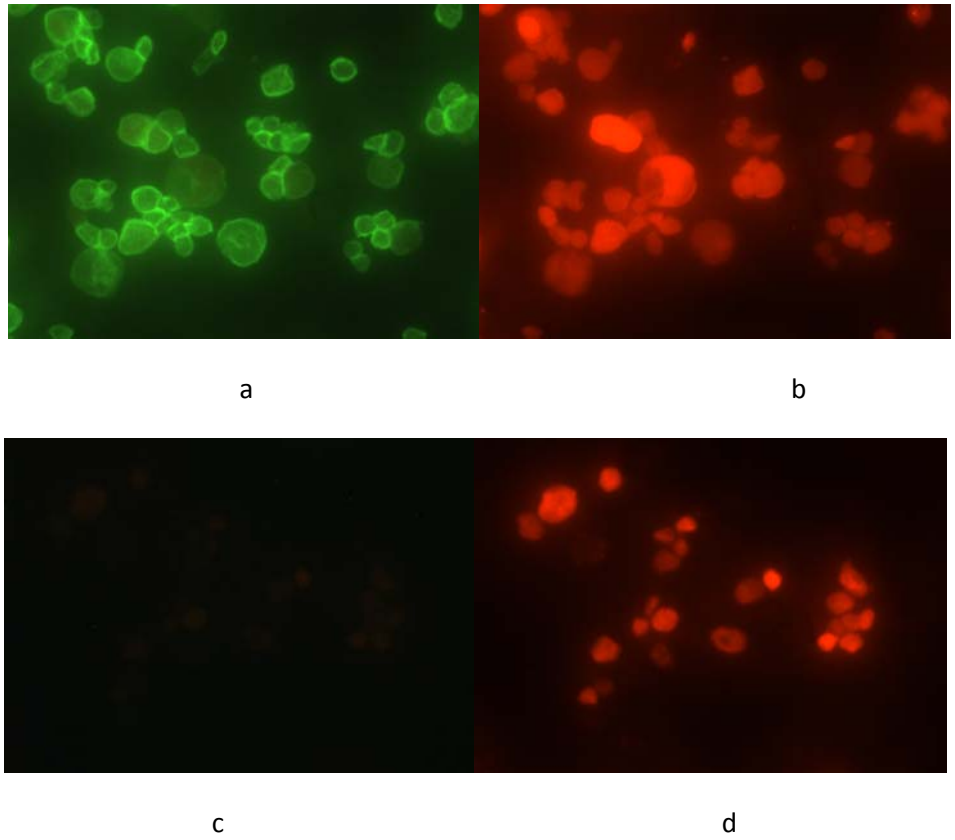

Fig.S2. Fluorescence microscope images showing: (a) target cells stained with Erbitux and (FITC-labelled) secondary antibodies, (b) red fluorescence of the target cells (which are mCherry transfected) from panel a, (c) target cells stained with only secondary antibodies, (d) red fluorescence of the cells from panel c.

Issue Highlights

Issue Highlights—March 2015

In their review Damuzzo et al. (1) focus on the correct identification of circulating and tumour-associated so-called myeloid-derived suppressor cells (MDSCs) in humans and mouse models. The reason to do this is because MDSCs are endowed with suppressive activity and because their expansion has been associated with disease progression and reduced survival. Because of their heterogeneous composition, accurate phenotyping of these cells will almost invariantly require a multicolour approach in order to allow appreciation of MDSC subsets.

Correct minimal residual disease (MRD) detection is crucial for therapy response assessment in a considerable number of hematologic disorders including mantle cell lymphoma (MCL) (2). Multiparameter flow cytometry (MFC) immunophenotyping is currently increasingly used to assess MRD in malignant disorders. Recently, a FACSCantoll (DB Biosciences, San Jose, CA)-based 7-color/8-antbody MFC approach has been published, allowing for the determination of MRD in multiple myeloma patients (3). Chovancova et al.(4) found that, although MCL presents high immunophenotypic variability, the combination of CD20/23/5/19/200/62 L/45 is very favourable in flow cytometric MRD measurement in MCL reaching a sensitivity of up to 2×10^{-4}. In another study, Mathis et al. (5) show that this protocol is transposable between harmonized $\geq$ 7-color instruments and that a homogeneous rapid MRD evaluation can be performed in most MFC platforms.

Although not all immunohistochemical techniques can easily be automated by image analytical systems, in a remarkable study Qin, Y et al. (6) concluded that a computerized delineation of nuclei in re-stained PAP smears with p16/ki67 can result in an automated high-throughput profiling method achieving accurate data.

Because cigarette smoke is a powerful producer of reactive oxygen species (7), hypothesized that spermatozoa of smokers would be at increased risk of having DNA fragmentation as compared to spermatozoa of non-smoking men. However, by applying a novel TUNEL assay coupled to a vitality marker (LIVE/DEAD®) the authors found no deleterious effect, i.e., increased DNA fragmentation, of smoking on spermatozoa. More studies concerning the potential mutagenic capacities of cigarette smoke on spermatozoa are mandatory.

Eidenschink Brodersen et al. (8), utilizing a NH_4Cl lysis protocol have defined various immunophenotypic abnormalities that indicate dyserythropoiesis in myelodysplastic syndromes. Preliminary studies also indicate strong correlation between phenotypic erythroid dysplasia and poor prognosis, as classified cytogenetically.

Perspectives from Didier G. Ebo.

It is well-known that the epidermal growth factor receptor (EGFR) is overexpressed in carcinoma and can be used as a therapeutic target. Levi et al. (9) developed a Bio-Ferrography method enabling isolating EGFR overexpressing carcinoma cells from human blood. Recovery values as high of 8% for 1 mL PBS and 53% for 1 mL whole blood, with a limit of detection of 30 and 100 target cells, respectively, were achieved. Further studies are warranted to assess whether this technique allows early diagnosis of EGFR overexpressing tumour types.

In MRD flow cytometry results can easily be confounded by (unknown) expression of markers on nearby

*Correspondence to: Didier G. Ebo, M.D., Ph.D., Department of Immunology - Allergology, University of Antwerp, Belgium.
E-mail: Didier.Ebo@ua.ac.be
Published online in Wiley Online Library (wileyonlinelibrary.com).
DOI: 10.1002/cyto.b.21230

cells. In their article Soma et al. (10) focuses on the expression of CD19 on NK cells. They conclude that it is an apparent but infrequent finding, not a consequence of technical error. More research to optimizing panels, combining techniques or using other specimens like bronchoalveolar lavage is needed.

Didier G. Ebo*
Department of Immunology - Allergology
University of Antwerp,
Belgium

LITERATURE CITED

1. Damuzzo V, Pinton L, Desantis G, Solito S, Mariqo I, Bronte V, Mandruzzato S. Complexity and challenges in defining myeloid-derived suppressor cells. Cytometry Part B 2015;88B:77–91.
2. Gaipa G, Basso G, Biondi A, Campana D. Detection of minimal residual disease in pediatric acute lymphoblastic leukemia. Cytometry Part B 2013;84B:359–369.
3. Robillard N, Bene MC, Moreau P, Wuilleme S. A single-tube multiparameter seven-colour flow cytometry strategy for the detection of malignant plasma cells in multiple myeloma. Blood Cancer Journal 2013;3:e134
4. Chovancova J, Bernard T, Stehlikova O, Salek D, Janikova A, Mayer J, Doubek M. Detection of minimal residual disease in mantle cell lymphoma. Establishment of novel 8-color flow cytometry approach. Cytometry Part B 2015;88B:92–100.
5. Mathis S, Chapuis N, Borgeot J, Maynadié M, Fontenay M, Béné MC, Guy J, Bardet V. Comparison of cross-platform flow cytometry minimal residual disease evaluation in multiple myeloma using a common antibody combination and analysis strategy. Cytometry Part B 2015; 88B:101–109.
6. Qin Y, Walts AE, Knudsen B, Gertych A. Computerized delineation of nuclei in liquid-based pap smears stained with immunohistochemical biomarkers. Cytometry Part B 2015;88B:110–119.
7. de Bantel A, Fleury-Feith J, Poirot C, Berthaut I, Garcin C, Landais P, Ravel C. Simultaneous vitality and DNA-fragmentation measurement in spermatozoa of smokers and non-smokers. Cytometry Part B 2015; 88B:120–124.
8. Eidenschink Brodersen L, Menssen AJ, Wangen J, Stephenson C, de Baca M, Zehentner B, Wells D, Loken M. Assessment of erythroid dysplasia by "difference from normal" in routine clinical flow cytometry work-up. Cytometry Part B 2015;88B:125–135.
9. Levi O, Shapira A, Tal B, Benhar I, Eliaz N. Isolating EGFR overexpressing carcinoma cells from human whole blood by bio-ferrography. Cytometry Part B 2015;88B:136–144.
10. Soma L, Wu D, Chen X, Edlefsen K, Fromm J, Wood B. Apparent CD19 expression by natural killer cells: A potential confounder for minimal residual disease detection by flow cytometry in B lymphoblastic leukemia. Cytometry Part B 2015;88B:145–147.